
Article:
Helm, C.W. orcid.org/0000-0001-7995-8809, Bateman, M.D. orcid.org/0000-0003-1756-6046, Carr, A.S. orcid.org/0000-0001-5794-6428 et al. (6 more authors) (2023) Pleistocene fossil snake traces on South Africa's Cape south coast. Ichnos: an International Journal of Plant and Animal Traces, 30 (2). pp. 98-114. ISSN 1042-0940

https://doi.org/10.1080/10420940.2023.2250062

Final published version is available at
https://www.tandfonline.com/doi/full/10.1080/10420940.2023.2250062?src=recsys
Supplementary data is presented at the end of this document

Title

Pleistocene fossil snake traces on South Africa's Cape south coast

Keywords

Aeolianite, puff adder, rectilinear motion, sidewinding, OSL dating

Authors

Charles W. Helm[1]* helm.c.w@gmail.com

Mark D. Bateman[2] M.D.Bateman@Sheffield.ac.uk

Andrew S. Carr[3] asc18@leicester.ac.uk

Hayley C. Cawthra[1,4] hcawthra@geoscience.org.za

Jan C. De Vynck[1,5] Jan.DeVynck@mandela.ac.za

Mark G. Dixon[1] ghostfishing@strandloperproject.org

Martin G. Lockley[1,6] martin.lockley@ucdenver.edu

Willo Stear[1] willos@tiscali.co.za

Jan A. Venter[1,7] Jan.Venter@mandela.ac.za

* Corresponding author: Charles Helm

Box 1690, Tumbler Ridge, BC, V0C 2W0, Canada

Phone +1 250 242 3984; Fax +1 250 242 49076; email helm.c.w@gmail.com

Affiliations

[1] African Centre for Coastal Palaeoscience, PO Box 77000, Nelson Mandela University, Gqeberha, 6031, South Africa.

[2] Department of Geography, University of Sheffield, Sheffield, S3 7ND, U.K.

[3] School of Geography, Geology and the Environment, University of Leicester, Leicester, LE1 7RH, UK.

Final published version is available at
https://www.tandfonline.com/doi/full/10.1080/10420940.2023.2250062?src=recsys
Supplementary data is presented at the end of this document

[4] Minerals and Energy Unit, Council for Geoscience, Western Cape regional office, PO Box 572, Bellville, 7535, South Africa.

[5] Evolutionary Studies Institute, University of the Witwatersrand, P Bag 3, WITS, 2050, Johannesburg, South Africa

[6] Dinosaur Trackers Research Group, Campus Box 172, University of Colorado Denver, PO Box 173364, Denver, 80217-3364, USA.

[7] Department of Conservation Management, George Campus, Nelson Mandela University, Madiba Drive, George, 6530, South Africa.

ABSTRACT

Snakes form a large, familiar and distinctive component of the world's reptile fauna, with a rich body fossil record stretching back to the Jurassic. The sparse, minimal and questionable evidence of snake traces in the ichnological record is therefore surprising. Extant snakes in southern Africa employ three types of locomotion – rectilinear, sidewinding and undulatory, all of which result in distinctive, recognizable traces. A site exhibiting convincing evidence of rectilinear motion, probably made by a puff adder, has been identified in Pleistocene aeolianites on South Africa's Cape south coast. A new ichnogenus and ichnospecies, *Anguinichnus linearis*, have been erected to describe this trace. A new suite of optically stimulated luminescence (OSL) ages from aeolianites from the De Kelders Cave locality, 1.4 km to the south, suggests that the site dates to ~93–83 ka. Trace fossil evidence of sidewinding and undulatory motion is more equivocal, and open to alternate interpretations.

Final published version is available at
https://www.tandfonline.com/doi/full/10.1080/10420940.2023.2250062?src=recsys
Supplementary data is presented at the end of this document

INTRODUCTION

Through the Cape south coast ichnology project, conducted under the auspices of the African Centre for Coastal Palaeoscience, Nelson Mandela University, more than 350 Pleistocene vertebrate ichnosites have been identified in coastal aeolianites and cemented foreshore deposits in the Western Cape Province, South Africa. Within the suite of mammal, avian and reptile sites, the latter have assumed disproportionate significance due to their palaeo-environmental implications. Examples include hatchling sea-turtle trackways (Lockley et al. 2019), crocodylian tracks and swim traces (Helm et al. 2020; Helm and Lockley 2021), and very large tortoise tracks and traces (Helm et al. 2023a).

Snakes (Class Reptilia, Order Squamata, Suborder Serpentes) form a large, familiar and distinctive component of the reptile fauna of southern Africa. They belong to nine families (Branch 2016) and are represented by between 168 (Branch 2016) and 151 species (Van den Heever et al. 2017).

As snakes are often encountered on modern coastal dune surfaces in the region, it is therefore surprising that their traces, which are distinctive, have not previously been identified on palaeosurfaces within the Cape coastal aeolianites. In this respect, the sparsity of snake traces in the global ichnology record is equally puzzling. By contrast, the body fossil record is rich, with snake fossils having been identified as far back as the Jurassic Period (Caldwell 2019; Caldwell et al. 2015). To the best of our knowledge, there are no published descriptions of fossil epifaunal snake traces in the global ichnological literature. In what appears to be the 'closest approach' Loope (2005) described abundant, sinuous trace fossils in Jurassic dune deposits in Utah, U.S.A. Ranging from 2–5 cm in diameter, they were interpreted as having been made by sand-swimming, elongate animals using lateral undulation (see below) to propel themselves through the sand. The makers of these

Final published version is available at
https://www.tandfonline.com/doi/full/10.1080/10420940.2023.2250062?src=recsys
Supplementary data is presented at the end of this document

infaunal trails may have been snakes or other creatures that were limbless or had reduced limbs. As detailed below, Braddy et al. (2003) recognised the sidewinder pattern in formal ichnotaxonomy (*Serpentichnus*), assigning the pattern to a Permian amphibian.

Other than larger-diameter burrows (at high angles to stratification) for which a snake origin is considerably less likely than that of other burrowing creatures (Loope 2006, 2008), the remainder of the global ichnology record of snakes appears to involve neoichnological fossorial observations (Kinlaw 1999; Himes 2000; White 2005; Deufel 2017) and experiments (Hembree and Hasiotis 2007). Such studies allow postulates to be made on what might be encountered in the trace fossil record, but do not contribute to this record. Our discussion in this article is restricted to surface (epifaunal) features, and does not include burrows or subsurface traces (infaunal traces) or scat.

The purpose of this article is to describe a recently identified ichnosite on the Cape coast, which can be attributed with confidence to a snake, and as such merits consideration as the first epifaunal snake trace from the fossil record. We then also consider three other sites that illustrate potential challenges in identifying epifaunal snake traces. In this regard it is possible that hitherto unidentified traces that might be of snake or other large amniote affinity have yet to be correlated with their trackmakers. We review the different types of locomotion of extant snakes in southern Africa, provide age estimates for the new ichnofossil sites, and address ichnotaxonomy.

SNAKE LOCOMOTION AND NEOICHNOLOGY

Among extant snakes in southern Africa there are three types of locomotion: rectilinear, sidewinding, and undulatory (Branch 1994; Liebenberg 2000; Stuart and Stuart 2019; Van den Heever et al. 2017). Reference works from other parts of the world likewise describe rectilinear and undulatory forms of snake motion (e.g., Martin 2013 – p. 365–369).

Final published version is available at
https://www.tandfonline.com/doi/full/10.1080/10420940.2023.2250062?src=recsys
Supplementary data is presented at the end of this document

Rectilinear ('caterpillar') locomotion

Rectilinear motion is employed by heavy, thick-bodied snakes such as the puff adder (*Bitis arietans*) or the African rock python (*Python sebae*). Making use of its weight, the snake uses its belly muscles to move its ventral scales, and grips areas of coarseness in the substrate with the posterior edges of the scales (Liebenberg 2000; Van den Heever et al. 2017). The snake is then drawn forwards through the muscular contractions, leaving a linear traceway (Fig. 1a). The rate of progression is relatively slow, and in order to move faster these snakes will employ undulatory movement, as described below (Liebenberg 2000). Slight undulations in the traceway usually imply slightly more rapid movement. A diagnostic feature, when present, particularly in the case of the puff adder (Liebenberg 2000), is a thin groove / drag mark in the centre of the trace, registered by the tail-tip (Fig. 1b). Such a drag-mark is often discontinuous. When fine detail is preserved, the ventral scales may leave closely-spaced transverse markings (Liebenberg 2000; Van den Heever 2017). Videos (recorded by one of us – MD) of puff adders employing rectilinear motion in the Garden Route National Park on the Cape south coast can be viewed at: https://youtu.be/iWZfIzIayDk and https://youtu.be/NVTHbTADepY .

Puff adders often adopt a coiled position, from which they lunge and strike. In such cases a 'hybrid' trace may be created, in which prominent lateral curved ridges are combined with a central tail-tip impression that indicates the direction of the strike and the direction followed (Fig. 1c).

Sidewinding locomotion

Sidewinding locomotion involves lifting most of the body from the sand while involving the body in smooth curls and undulating motion. This results in a highly distinctive series of parallel traces, each

Final published version is available at
https://www.tandfonline.com/doi/full/10.1080/10420940.2023.2250062?src=recsys
Supplementary data is presented at the end of this document

of which may appear slightly sinuous, and which may sometimes even record a head impression at one end (Fig. 1d). Each trace lies at an angle to the direction of motion. This form of locomotion enables swift travel over hot dunes, and is limited in southern Africa to a small adder (Péringuey's adder – *Bitis peringueyi*) on dune slopes in the Namib Desert (Fig. 1e).

Undulatory ('serpentine') locomotion

This is the most common form of locomotion, and is often associated with snakes, hence the alternative name, 'serpentine'. It involves sinuous movement, whereby forward propulsion is enabled through a series of sideways motions, pressing different parts of the body in waves against stones, uneven areas in the ground, or vegetation. In so doing a reaction force is generated, which creates forward thrust. The result is a wavy, sinuous pattern. In sandy substrates tiny walls of sand are pushed up outside the outer curves, and form a distinctive feature when present (Van den Heever et al. 2017). In most cases, identification to tracemaker species level is not possible (Fig. 1f). Small undulatory snake traces cannot be distinguished from traces of legless lizards (a group characterised also by the creation of shallow subsurface undulatory burrow traces (Stuart and Stuart 2019).

The ascent of inclined surfaces is a challenge for all three forms of locomotion, and is influenced by inclination of slope and direction of travel relative to slope. Puff adders and pythons resort to undulatory motion (Fig. 2). Sidewinding snakes are forced to reduce the distance between successive trace-making motions on dune slopes, and slumping of dune sediment may occur. Snakes that usually employ undulatory motion increase the frequency of undulations. In contrast, downslope travel is easier, and undulations often decrease or even disappear. Such findings assist in determining the direction of travel (Van den Heever et al. 2017).

Final published version is available at
https://www.tandfonline.com/doi/full/10.1080/10420940.2023.2250062?src=recsys
Supplementary data is presented at the end of this document

GEOLOGICAL CONTEXT

Pleistocene ichnofossils occur in aeolianites and cemented foreshore deposits along the Cape south coast of South Africa (Figure 3). These deposits are the consolidated remains of, inter alia, ancient sand dunes, inter-dune surfaces, lagoonal environments and beaches. Track-bearing aeolianites occur within the Waenhuiskrans Formation (Malan 1989,) whereas those in foreshore and lagoonal deposits are contained within the Klein Brak Formation (Malan 1991). The two formations form part of the Cenozoic Bredasdorp Group.

When originally formed, the ichnosites would have been situated at the margin of the Palaeo-Agulhas Plain, most of which is currently submerged. Pleistocene sea-level oscillations led to substantial variability in the exposure of the Palaeo-Agulhas Plain and the position of the palaeo-shoreline (Cawthra et al., 2020; Marean et al. 2020). At ~91 ka, for example, sea levels were 45 m lower than the present and the coastline at Walker Bay was ~8-10 km seaward of today's coast, whereas at ~79 ka, sea levels were ~25 m lower than at present, and the coastline was ~2 km from parts of today's coast (Waelbroeck et al., 2002). Further to the east, in the vicinity of Sites 2 and 3, described below, at ~91 ka the coastline was as much as 60 km seaward of today's coast (Cawthra et al., 2014; Fisher et al., 2010). In contrast, during the Marine Isotope Stage (MIS) 5e sea-level high-stand, at ~126 ka, the sea level was 6–8 metres higher than at present (Carr et al. 2010).

The aeolianites and cemented beach deposits mostly comprise fine-to medium-grained, quartz-dominated clastic sandstones containing calcium carbonate derived mainly from marine shells. The calcium carbonate cement varies from predominantly sparite in the dune deposits to micrite in the beach deposits. Although they are frequently referred to as calcarenite rocks, they generally contain

Final published version is available at
https://www.tandfonline.com/doi/full/10.1080/10420940.2023.2250062?src=recsys
Supplementary data is presented at the end of this document

less than 20% calcium carbonate cement. Globally, aeolianite (wind-deposited calcarenite) deposits are common in mid-latitude regions, typically between 20° and 40° (Brooke 2001). Aeolianites are sensitive palaeoenvironmental indicators, providing insights into palaeo-wind directions through their orientations and geometry, as well as preserving palaeontological and archaeological materials (Roberts et al. 2013).

Several factors contribute to the formation of high-anatomical-fidelity Pleistocene ichnofossils on the Cape south coast. A moist substrate is considered paramount, and the finest-grained sediments have the highest potential to yield tracks of optimal quality (Helm 2023). Surface tension, cohesion between sand grains and surface slope angle are other important variables (Helm 2023). Roberts and Cole (2003) attributed the plentiful occurrence of ichnosites in the Cape coastal aeolianites to a combination of (i) the cohesiveness of moist sand upon which the tracks and traces were initially made, which provides an effective moulding agent; (ii) high sedimentation rates, which promote swift burial of the trace fossils once they were formed; (iii) rapid cementation and lithification via partial solution and re-precipitation of bioclasts ,and (iv) shoreline erosion, which re-exposes the trace fossil-bearing surfaces.

Some of the palaeosurfaces on the Cape south coast containing ichnofossils with the highest anatomical fidelity display a thin crust or 'veneer' of fine-grained material. It is possible that surface cohesion of the track-bearing substrate may have been enhanced through the binding of moist sand grains by microbial activity similar to that described by Seilacher (2008), and/or by surface evaporation, creating a thin evaporite crust. Such a veneer may seal a surface soon after track formation and preserve detail before burial, and may facilitate the subsequent separation of layers to reveal the palaeosurfaces.

MATERIALS AND METHODS

Final published version is available at
https://www.tandfonline.com/doi/full/10.1080/10420940.2023.2250062?src=recsys
Supplementary data is presented at the end of this document

The four ichnosites (which are shown in Fig. 3) were named Site 1, Site 2, Site 3 and Site 4, in order from west to east. Global Positioning System readings were taken at each site, using a hand-held device. Locality data were reposited with the African Centre for Coastal Palaeoscience at Nelson Mandela University. These are available to researchers upon request.

Photographs were taken at sites 1, 2 and 4. Site 1 was visited five times, during different lighting conditions and with differing tidal conditions and algae coverage. The specimen from Site 3 was examined as part of the collections of the Blombos Museum of Archaeology in Still Bay.

For rectilinear patterns, measurements included trace length and width. The presence or absence of a central groove was noted. For the sidewinding pattern, distance between diagonal grooves and ridges was measured, as well as the length of these features, and the orientation relative to the longitudinal axis of the trace. For the undulatory pattern, width, amplitude ('external straddle') and wavelength ('crest-to-crest distance') were measured. Results were recorded in centimetres and degrees.

Photogrammetric analysis was not feasible at Site 4, but was applied to the specimens from sites 1, 2 and 3, *sensu* Matthews et al. (2016). 3D models were generated with Agisoft Metashape Professional (v. 1.0.4) using an Olympus Tough model TG-6 camera (focal length 4.5 mm; resolution 4000 x 3000; pixel size 1.56 x 1.56 um). The final images were rendered using CloudCompare (v.2.10-beta).

In ichnological parlance, the term 'track' is often used synonymously with 'print' or 'footprint', suggesting a tetrapod (quadruped or biped) vertebrate origin. 'Trackway', likewise, is used to denote a discontinuous sequence of tracks made by a single animal. It seems inaccurate to use the terms

Final published version is available at
https://www.tandfonline.com/doi/full/10.1080/10420940.2023.2250062?src=recsys
Supplementary data is presented at the end of this document

'track' and 'trackway' in the absence of individual footprint features; for example, traces of fishes are not generally referred to as 'tracks' (e.g., Anderson 1976). In invertebrate ichnology the term 'traceway' or 'trail' may be used, even (by some authors) when tiny tracks are present. The term 'trail', with its connotation of a surface pathway (or with surface disturbances of sediment registered by body parts other than feet or limbs), can also be used to denote a feature made by a single 'trailmaker'. Recognising these issues, we have chosen to use the terms 'trace' and 'traceway' to describe surface features registered by snakes, best known from neoichnology: i.e., while made by tracemakers that are technically tetrapods they lacked quadrupedal morphology, and thus could not register individual tracks.

RESULTS AND INTERPRETATION

Site 1 - Walker Bay Nature Reserve

A large, loose slab containing ichnological features was identified on the coastline in the Walker Bay Nature Reserve in 2022 (Fig. 4a). The slab, measuring 3.0 m in maximum length, 2.6 m in maximum width, and approximately 0.4 m in thickness, must have become dislodged from overlying aeolianite cliffs. At the time of discovery its surface was bare and appeared to be freshly exposed, although it was submerged at high tide. Three weeks later it was covered in a thin layer of algae and sand (Fig. 4b). At a subsequent visit five weeks later it was fully covered by sand. When the surface was bare, the most obvious feature was a large-bovid trackway containing four complete tracks and one partial track (at the edge of the surface) in concave epirelief (Fig. 4c, Fig. 4d). Due to overprinting, some of these appeared as 'doubles', with one track adjacent to and partially covering a track beside it. The tracks appeared consistently wider than they were long: ~13 cm long and ~17 cm wide, with a pace length of ~75 cm.

However, a more subtle feature was present, forming a long, shallower, mostly straight (but slightly sinuous in places) furrow, 2.8 m in length and varying from 6–9 cm in width. In places a central groove and ridge were evident (Fig. 5a). In one area one of the bovid tracks impinged on and slightly deformed the linear furrow (Fig. 5b). When the surface was covered in algae and sand, the narrow central groove was accentuated at the southern end of the slab (Fig. 5c). Figure 5d is a 3D photogrammetry image of this traceway.

We confidently attribute the large-bovid trackway to the extinct long-horned buffalo (*Syncerus antiquus*); we have previously reported that no extant bovids in southern Africa routinely register tracks that are significantly wider than they are long (Helm et al. 2018). The area where one of the tracks is superimposed on and slightly deforms the furrow indicates that the furrow was registered before the long-horned buffalo tracks, and thus excludes a diagenetic cause or more recent erosional cause for the furrow. The dimensions of the furrow and its slightly sinuous form point to a large snake employing predominantly rectilinear motion as the tracemaker. The central groove and ridge occurrences are consistent with a tail-tip impression, further confirming this interpretation. A puff-adder (*Bitis arietans*) is regarded as the likeliest tracemaker. Puff adders are heavy, thick-set snakes with a reported average length range of 70–90 cm, and a maximum length of 120 cm (Branch 1994).

Site 2 – Geelkrans Nature Reserve

A curved furrow, 60 cm in length and ~9 cm in width, occurs on a loose south-facing aeolianite slab at the high tide mark in the Geelkrans Nature Reserve, east of Still Bay (Fig. 6). It exhibits an eroded, raised rim on each side. The amount of curvature is not consistent along the length of the feature, being greater in the left (western) portion. Diagnostic features such as a narrow central (tail-tip) groove are not evident. No other tracks or traces are evident on the surface.

Final published version is available at
https://www.tandfonline.com/doi/full/10.1080/10420940.2023.2250062?src=recsys
Supplementary data is presented at the end of this document

A longer specimen would be desirable, along with diagnostic features such as a central groove or sinuosity. There are no associated animal tracks to suggest that an object was dragged along the dune surface, and the presence of rims excludes the possibility of an origin involving two rocks recently grinding against each other. Although alternative explanations do not readily come to mind, and the morphological dimensions are consistent with a *B. arietans* trace representing mostly rectilinear locomotion, the evidence cannot be considered conclusive. Site 2 is interpreted, therefore, as a possible but inconclusive snake-trace site.

Site 3 – Bosbokfontein Nature Reserve

As part of a survey for ichnosites an extremely thin, fragile rock was recovered from near the high tide mark on the coast of the private Bosbokfontein Nature Reserve. The western boundary of this private reserve is contiguous with the eastern boundary of the Geelkrans Nature Reserve (Fig. 7a, 7b). Site 3 is situated 1.5 km east of Site 2. The specimen is reposited in the Blombos Museum of Archaeology in Still Bay (accession number ICH 002 AN). It measures 35 cm in maximum length and 30 cm in maximum width. Its thickness is as little as 1.5 cm in places, with a maximum of 2.8 cm. The fossil trace extends for the length of the rock specimen, i.e., 35 cm). This unusual feature consists of a series of twelve evenly spaced, parallel diagonal ridges, aligned at ~45° to the main longitudinal axis, and separated by grooves. The alternating diagonal ridges and grooves are consistent and repetitive in form, and appear relatively straight or display slight convexity. Half of the main longitudinal axis of the trace is formed by a furrow (~3 cm wide) and the other half by a ridge (also ~ 3 cm wide). The furrow and ridge, 6 cm wide in total, exhibit slight sinuosity, and appear to slightly distort the alternating diagonal grooves and ridges. The diagonal grooves and ridges thus create alternating raised and depressed areas within the longitudinal furrow, and bumps and troughs along

the longitudinal ridge. In places, the diagonal grooves and ridges are faintly evident in extension beyond the outer margin of the longitudinal ridge, with a maximum length of 13 cm.

The features are interpreted in epirelief (concave and convex). No comparable surface neoichnological pattern on modern dunes and beaches has been identified on the Cape coast or indeed anywhere else in South Africa. A wide net thus needs to be cast in order to explain the noted features, including extralimital vertebrate candidates and invertebrate tracemakers. One possibility to account for the parallel diagonal features is a traceway made through sidewinder motion, exemplified by that of Péringuey's adder (*Bitis peringueyi*), also known as Péringuey's desert adder or the desert sidewinding adder. Although the spaces between the features seem less than what is typically recorded on a level surface by this snake, when such small desert-dwelling adders ascend a slope, the successive traces become more closely spaced. Furthermore, the longitudinal furrow and adjacent longitudinal ridge suggest that such a snake may have moving diagonally up a slope, so that some sand was shifted downslope (forming the longitudinal furrow and ridge), slightly distorting the traces. The current southern African distribution of sidewinding adders is restricted to *Bitis peringueyi* on sand dunes in the Namib Desert, from southern Namibia to southern Angola (Branch 1994).

Branch (1994) describes *Bitis peringueyi* as a very small adder, 20—25 cm in length, with young measuring as little as 8-11 cm in length. The recorded dimensions of the possible fossil traceway, with a maximum length of 13 cm for some traces, are thus not inconsistent with this species, which often shuffles into the sand, leaving only the eyes exposed; sometimes the black tail tip is also exposed, and waved to attract prey (Branch 1994).

Final published version is available at
https://www.tandfonline.com/doi/full/10.1080/10420940.2023.2250062?src=recsys
Supplementary data is presented at the end of this document

However, an alternative explanation is plausible. Minter et al. (2008) described *Augerinoichnus helicoidalis*, a new helical burrow trace fossil from non-marine Permian deposits in New Mexico (Fig. 8). It comprised 'linear successions of regularly repeated horseshoe-shaped structures, although the individual horseshoe-shaped structures are consistently offset to one side relative to the preceding horseshoe-shaped structure' (Minter et al. 2008 - p. 1201, morphotype 1). In some of the examples provided (their figure 3.2 and figure 3.3, our Figure 8) these structures are associated with a straight horizontal trace, which runs approximately parallel to the succession of horseshoe-shaped structures, and curves slightly towards one end. In many ways this resembles the Site 3 specimen, although *Augerinoichnus helicoidalis* is somewhat smaller.

Minter et al. (2008) postulated that the original helical-shaped burrow was infaunal and horizontal, with tight coiling which was oblique to the main axis of the burrow in the horizontal plane. Through deflation, part of the burrow would become exposed on the surface, leaving a horizontal plane preserving a succession of horseshoe-shaped, nested hollows. It was thought that *Augerinoichnus* was most likely produced by a vermiform animal.

The well-known helical burrow *Diamonelix*, attributed to a Miocene beaver, is always vertical and much larger (~30 cm) than *Augerinoichnus helicoidalis* (Martin and Bennett, 1977). It cannot be confused with any of the other traces discussed herein.

Braddy et al. (2003) erected the ichnogenus *Serpentichnus robledoensis* to describe a series of repeated swimming traces in Permian deposits in New Mexico (Fig. 9). These traces, a series of L-shaped grooves, resembled those made by sidewinding snakes, and were assigned to amphibians, in particular the lysorophian *Brachydectes*. Lysorophians were long bodied, snake like amphibians, with diminutive or absent limbs; i.e., the sidewinder pattern has already been recognized in formal

ichnotaxonomy. Braddy et al. (2003) concluded that sidewinding was adopted as a means of locomotion long before it evolved in snakes. Minter and Braddy (2009) described a second ichnospecies, *S. sigmoidalis*.

Site 4 – Robberg Nature Reserve

The Island on the Robberg Peninsula is an area rich in fossil tracksites (Helm et al. 2019). In one portion of this area, large aeolianite blocks have fallen down from the cliffs above, and have come to rest above the high tide mark (Fig. 10a). Our attention was drawn to one of these blocks containing an enormous track feature in hyporelief. Measuring 85 cm in length and at least 55 cm in width, it was a composite of three large elephant tracks. In an adjacent crevice other features were evident in convex hyporelief. One of these features, ~1 cm in width, exhibited an undulatory pattern over a distance of 45 cm (Fig. 10b). Three wavelengths ('crest-to-crest' distances) could be measured, each of which is ~9 cm. The amplitude ('external straddle') is ~2 cm, yielding a wavelength/amplitude ratio of 4.5.

To enable confident identification, a longer undulating feature would be desirable. Typical features of undulatory-pattern snake traces such as evidence of mounds of sand being pushed up lateral to the convex margins are absent. Although the undulating pattern is indisputable, and the dune palaeoenvironment precludes an identification of other undulating patterns such as *Undichna* or *Cochlichnus*, other causes cannot be excluded. It is not inconceivable that a millipede, caterpillar or small lizard happened to create a trace that exhibits a few undulations, and that the relatively poor preservation does not allow identification of diagnostic features such as footprints. Site 4 can thus be regarded, at best, as a possible snake-trace site, and an indication of what to search for in future.

ICHNOTAXONOMY

Final published version is available at
https://www.tandfonline.com/doi/full/10.1080/10420940.2023.2250062?src=recsys
Supplementary data is presented at the end of this document

Preamble

It appears that snake traces have not been assigned a formal ichnogenus or ichnospecies name. However, ichnogenera have been assigned to other fossil undulatory patterns, which have been extensively reported on, e.g., *Undichna* and *Cochlichnus*.

The ichnogenus *Undichna* was erected by Anderson (1976) in describing a number of Permian ichnosites in South Africa. *Undichna* traces are made by the pectoral, pelvic, caudal and anal fins of fish. The ichnogenus was formally revised by Minter and Braddy (2006), reducing the number of valid ichnospecies to nine.

Cochlichnus describes a small, sinuous trace that resembles a sine curve. It is found in aquatic settings.

Aquatic annelids, insect larvae, and nematodes have been postulated as tracemakers (Hasiotis and Bown 1992). Uchman et al. (2004), in determining the morphometric parameters of *Cochlichnus anguineus*, examined the ratio between wavelength (w) and amplitude (a). The ratio varied considerably between 'tight forms' and 'stretched forms', with a clear peak between 2.5 and 3.0.

Other traces exhibiting undulatory patterns have been assigned to *Lunichnium* (Turek, 1989) and *Batrachichnium* (e.g. Braddy et al. 2003). The former is characterised by paired tail impressions, and the latter contains tracks in addition to an undulatory trace, hence neither is discussed further here.

The example at Site 4 of a possible undulatory fossil snake trace on an aeolianite surface raises the inevitable question of whether a new ichnogenus would need to be introduced if less equivocal sites are identified. Strictly speaking the important criteria are whether the traces are unique: i.e., easily

differentiated from previously reported traces according to recognizable morphological features. As noted above, the long trace shown in Figure 4 and Figure 5 from Site 1 meets this criterion of uniqueness, despite the existence of other well-known undulatory traces such as *Undichna* and *Cochlichnus*. We therefore consider the trace from Site 1 to be distinctive enough to warrant a formal ichnotaxonomic description.

Formal ichnotaxonomy

Anguichnus ichnogen. nov. Figs. 4 and 5.

Holotype: Specimen from Site 1 in Figures 4 and 5.

Type locality: Site 1, north of De Kelders in Walker Bay Nature Reserve.

Type horizon: the Pleistocene Waenhuiskrans Formation.

Derivation of ichnogenus name: *Angui*, from the Latin '*anguis*' meaning 'snake', *ichnos* meaning 'trace'.

Differential diagnosis. Large rectilinear, slightly undulating surface trace expressed as a shallow furrow up to 9 cm wide. A thin central groove occurs sporadically in or near the midline of the furrow. This differs from other undulatory traces attributed to vertebrates and invertebrates in width of trace, markedly greater wavelength (w) and lesser amplitude (a) of undulations if they are present: i.e., generally very low a/w values.

Anguichnus linearis ichnosp. nov.

Holotype: as for ichnogenotype. (Specimen shown from Site 1 in Figure 5).

Type locality: as for ichnogenotype. (Site 1, north of De Kelders in Walker Bay Nature Reserve).

Type horizon: as for ichnogenotype. (The Pleistocene Waenhuiskrans Formation).

Final published version is available at
https://www.tandfonline.com/doi/full/10.1080/10420940.2023.2250062?src=recsys
Supplementary data is presented at the end of this document

Derivation of ichnospecies name: *linearis* meaning 'linear'.

Description: a rectilinear, shallow furrow trace, up to 9 cm in width, with a thin, central, discontinuous groove possibly flanked by low ridges. Slight sinuosity may be discernable in the overall linear pattern. Length of trace is indeterminate.

Ichnotaxonomic discussion

Anguichnus linearis shares three features in common with the sinuous / undulatory traces *Undichna* and *Cochlichus*:

- they represent Repichnia (locomotion traces);
- they are surface traces;
- they have indeterminate lengths which are not ichnotaxonomically diagnostic.

Differences include the fact that *Undichna* represent subaqueous traces, universally attributed to fish. *Undichna* may be represented by single sinuous undulatory traces, representing single fin traces, but in many cases are represented by multiple in phase / out of phase traces representing registration by multiple fins. Thus, *Undichna* traces are also variable in size, wavelength and amplitude (w>a, w=a and w<a) with individual fin traces typically being very narrow. *Cochlichnus* traces are universally attributed to invertebrates such as nematodes and are associated with wet fine-grained sediments. They are also generally very small with very narrow furrows and regular wavelength and amplitude similar (w~=a).

Clearly *Anguichnus* exhibits a very subtle undulatory pattern with wavelength many times greater than amplitude. However, with only one (holotype) example it is possible to infer that similar traces attributed to snakes engaged in rectilinear motion might have greater a/w values as suggested by modern examples (Fig. 1b), and in some cases may approach zero (Fig. 1a). Modern examples also

Final published version is available at
https://www.tandfonline.com/doi/full/10.1080/10420940.2023.2250062?src=recsys
Supplementary data is presented at the end of this document

suggest that in cases with high-quality preservation in suitable sediments, closely-spaced transverse markings may be apparent.

DISCUSSION

We are confident in our interpretation of the features at Site 1 as representing the traceway of a snake employing rectilinear motion, most likely a puff adder or similar Pleistocene viper. The features at Site 2 perhaps suggest a similar phenomenon, although less conclusively.

The unprecedented pattern (for the region) seen at Site 3 is obviously intriguing. Neither explanation (sidewinding adder or helical burrow trace such as *Augerinoichnus*) is entirely satisfactory. The need to invoke slumping of sand to postulate a sidewinding adder trace is not parsimonious. A cautious approach seems warranted, in which both possibilities are considered plausible, while the search for similar specimens continues and alternatives are considered. If unequivocal fossil sidewinding traces are identified in future, they could possibly be assigned to *Serpentichnus*, although palaeo-environmental factors (e.g., unequivocal sub-aerial versus sub-aqueous registration of traces) might influence such ascription. The relatively poor preservation at Site 4 precludes a definite identification, although a snake employing undulatory motion is a plausible explanation, and a snake resting trace is a possibility.

In considering traces in aeolianites registered by snakes employing rectilinear motion, care needs to be taken to distinguish them from other long, linear or curvilinear features. Longitudinal grooves made by an object being dragged along the surface may also contain central striations (small grooves and ridges), which may be confused with a central tail-tip groove. A surface exposure of adequate size is required. In the case of humans dragging a stick or other item, or carnivores dragging prey, adjacent tracks, in the same orientation as the linear groove, should be present. (In the case of Site

Final published version is available at
https://www.tandfonline.com/doi/full/10.1080/10420940.2023.2250062?src=recsys
Supplementary data is presented at the end of this document

1, the trackway is aligned oblique to the snake trace, and was registered after it.) Elephant trunk drag impressions could potentially be a source of confusion, but typically appear on either side of an elephant trackway (Helm et al. 2021). Likewise, tetrapod tail-drag traces or toe-drag traces are typically associated with well-defined trackways (Kim and Lockley 2013): i.e., isolated tail traces are rarely if ever reported. Rhizoliths (Klappa 1980; Durand et al. 2018) may be surprisingly long and straight, but usually taper if they can be viewed over sufficient distance, and often alter the composition of the surrounding rock. Diagenetic and post-exposure factors need to be considered, although in the case of Site 1 this can be confidently excluded as the registration of the snake trace is seen to precede that of the long-horned buffalo trackway.

The absence of any previous compelling examples of surface snake traces in the global fossil record suggests that there may be as-yet-unknown biases against the preservation of such traces. The absence of unequivocal undulatory traces registered by snakes in Cape coastal aeolianites might reflect:

- our focussing on tracks to the exclusion of other patterns;
- a preference by snakes for avoiding open sand dunes and preferring vegetated areas,
- traces being shallow, faint, and difficult to detect, possibly in part as the weight of the snake may be distributed over its entire length – Figure 1f illustrates the minimal traces left immediately following the passage of a large, 1.5 m long mole snake (*Pseudaspis cana*).
- difficulty in recognizing patterns due to poor preservation of traces – this is related to sediment grain size, as Cape coastal dunes and beaches are characterized by relatively coarse-grained sediments, and preservation is superior in finer-grained sediments.

Dating

Final published version is available at
https://www.tandfonline.com/doi/full/10.1080/10420940.2023.2250062?src=recsys
Supplementary data is presented at the end of this document

None of the sites have been directly dated. However, dated sites nearby can be used to provide an approximate indication of the age of the deposits. Site 1 is clearly the most important, as it provides the most unequivocal evidence of a snake trace. To provide an age estimate for this site we were able to make use of existing, but hitherto unpublished, optically stimulated luminescence (OSL) ages from aeolianites around the De Kelders Cave site, ~1.4 km south of Site 1 (Fig. 11). The details of the sample locations, and the OSL dating methodology and results, are presented in the Supplementary Information. The resulting ages, which cover nearly the full depth of exposed aeolianite in this locale (Fig. S1), span an age range of 93 ± 6 ka – 83 ± 6 ka (Table 1). They imply a marine isotope stage (MIS) 5c/5b age range, consistent with exposures to the east near to Cape Agulhas (Carr et al., 2010) and ages typically obtained elsewhere along the Cape south coast (Bateman et al., 2011).

Additionally, through our recent OSL dating program, deposits 3.5 km east of Site 2 and 2 km east of Site 3 were dated to 134 ± 9 ka (Leic 21008 in Helm et al. 2023a). Aeolianites on the Robberg Peninsula were previously dated to late Marine Isotope Stage (MIS) 3 (Carr et al. 2019). Deposits within 30 m of the possible snake trace were shown to date to 56 ± 5 - 43 ± 4 ka (Table S1 in Helm et al. 2023b). Collectively, the sites therefore span an age range from MIS 5e (or terminal MIS 56) through MIS 3.

Palaeoenvironmental implications

The inferred puff adder traces at Site 1 (and possibly at Site 2) do not provide palaeoenvironmental inferences, other than indicating that this species inhabited the region in the Pleistocene, as it does today. A python tracemaker cannot be excluded, but the size is small for a python and, given the more subtropical and tropical distribution of the African rock python, a puff adder origin is much more likely. Furthermore, the central tail-tip drag is more characteristic of a puff adder than a python (Liebenberg 2000; Van den Heever 2017).

Final published version is available at
https://www.tandfonline.com/doi/full/10.1080/10420940.2023.2250062?src=recsys
Supplementary data is presented at the end of this document

The situation is different in the case of the possible sidewinder trace. There are no snakes capable of this mode of locomotion in South Africa today, and the only species in southern Africa is restricted to the Namib Desert. The situation is perhaps analogous to that of the sand-swimming golden mole (*Eremitalpa granti*), also known as the Namib mole. Trails indicative of Pleistocene sand-swimming golden moles were found on the Cape south coast (Lockley et al. 2021). It was concluded that either *E. granti* enjoyed a much wider distribution during the Pleistocene, or other, now extinct, sand-swimming golden moles had inhabited the dune fields of the Cape south coast. Either way, the presence of substantial dune fields was inferred (Lockley et al. 2021). Similar considerations might apply if the trace fossil at Site 3 represents sidewinding locomotion.

Assuming that the identification of a sidewinding trace at Site 3 is plausible, then either *Bitis peringuey* enjoyed a much wider distribution in the Pleistocene, or else a previously unsuspected, extinct, small sidewinding snake inhabited extensive dune fields on the Cape south coast during the Pleistocene. However, the alternative explanation of an invertebrate trace similar to that of *Augerinoichnus* illustrates the need for caution when interpreting this trace fossil.

CONCLUSIONS

The ichnosite identified in the Walker Bay Nature Reserve, probably from an age of ~93–83 ka, is interpreted as exhibiting the first palaeoichnological evidence of a surface trace registered by a snake, probably a puff adder. *Anguichnus linearis* ichnogen. et ichnosp. nov. gives a formal ichnotaxonomic label to this trace, presently known from a single example.

There are limited palaeoenvironmental implications resulting from this discovery. However, if further fossil evidence of a sidewinding adder on the Cape south coast is forthcoming, this would indeed have substantial implications, as sidewinders are currently restricted to Namib Desert dune

fields. The sidewinding pattern has already been recognized as *Serpentichnus*, although this was not registered by a snake.

The prevalence of traces of extant snakes on dunes in the region suggests that further fossil traces may be encountered in suitable Pleistocene deposits (probably from a range of ages) provided the relevant patterns are sought and recognized. The identification of the Walker Bay ichnosite can act as a spur to further exploration of Pleistocene aeolianites on the South African coast, in the hopes of helping to fill a substantial gap in the global palaeoichnology record.

ACKNOWLEDGEMENTS

We thank the following for their much appreciated assistance and support: Graham Avery, Given Banda, Simon Braddy, Jack Carrigan, Murray Gingras, Carina Helm, Linda Helm, Nic Minter, Niekie Rust, Renée Rust, John Ward, CapeNature staff; Gillian Maggs, Eugene Marais and Scott Turner of the Gobabeb Research and Training Centre; Michael Lutzeyer, Sean Privett and staff of Grootbos Nature Reserve.

The late Dr Dave Roberts originally mapped the aeolianites within the De Kelders Cave area, and provided the stratigraphic logs presented in Figure S2. Graham Avery is thanked for providing access and guidance during the acquisition of OSL sample Shfd05025 in 2005.

REFERENCES

Anderson, A. 1976. Fish trail from the Early Permian of South Africa. *Palaeontology*, 19: 397–409.

Final published version is available at
https://www.tandfonline.com/doi/full/10.1080/10420940.2023.2250062?src=recsys
Supplementary data is presented at the end of this document

Braddy, S. J., Morrissey, L. B., and Yates, A. M. 2003. Amphibian swimming traces from the Lower Permian of southern New Mexico. *Palaeontology,* 46(4): 671–683.

Branch B. 1994. *Field guide to the snakes and other Reptiles of Southern Africa*. Cape Town, Struik, 326 pp.

Branch B. 2016. *Pocket Guide Snakes and other Reptiles of Southern Africa*. Cape Town, Struik Nature, 160 pp.

Brooke, B. 2001. The distribution of carbonate eolianite. *Earth-Science Reviews*, 55: 135–164.

Caldwell, M. C. 2019. *The Origin of Snakes: Morphology and the Fossil Record*. CRC Press, 299 pp.

Caldwell, M., Nydam, R., Palci, A., and Apesteguía, S. 2015. The oldest known snakes from the Middle Jurassic-Lower Cretaceous provide insights on snake evolution. *Nature Communications,* 6: 5996. https://doi.org/10.1038/ncomms6996

Carr, A. S., Bateman, M. D., Roberts, D. L., Murray-Wallace, C. V., Jacobs, Z., and Holmes, P. J. 2010. The last interglacial sea-level high stand on the southern Cape coastline of South Africa. *Quaternary Research,* 73: 351–363.

Carr, A. S., Bateman, M. D., Cawthra, H. C., and Sealy, J. 2019. First evidence for onshore marine isotope stage 3 aeolianite formation on the southern Cape coastline of South Africa. *Marine Geology,* 407: 1–15.

Cawthra, H. C., Bateman, M. D., Carr, A.S., Compton, J. S., and Holmes, P. J. 2014. Understanding Late Quaternary change at the land–ocean interface: a synthesis of the evolution of the Wilderness coastline, South Africa. *Quaternary Science Reviews,* 99: 210–223.

Cawthra, H.C., Frenzel, P., Hahn, A., Compton, J.S., Gander, L. and Zabel, M., 2020. Seismic stratigraphy of the inner to mid Agulhas bank, South Africa. Quaternary Science Reviews, 235, p.105979.

De Cauwer, V. 2007. Mapping of the BCLME shoreline, shallow water and marine habitats. Final report for the BCLME project BEP/BAC/03/02.

Deufel, A. 2017. Burrowing with a kinetic snout in a snake (Elapidae: *Aspidelaps scutatus*). *Journal of Morphology,* 278: 1706–1715.

Durand, N., Monger H. C., Canti, M. G., and Verrecchia, E. P. 2018. Calcium Carbonate Features In Stoops, G., Marcelino, V., and Mees, F. (eds.), *Interpretation of Micromorphological Features of Soils and Regoliths* (Second Edition), Elsevier, pp. 205–258. https://doi.org/10.1016/B978-0-444-63522-8.00009-7

Fisher, E. C., Bar-Matthews, M., Jerardino, A., and Marean, C. W. 2010. Middle and Late Pleistocene paleoscape modeling along the southern coast of South Africa. *Quaternary Science Reviews.* 29: 1382–98.

Galbraith, R. F., Roberts, R. G., Laslett, G. M., Yoshida H., and Olley, J. M. 1999. Optical dating of single and multiple grains of quartz from Jinmium rock shelter, northern Australia, part 1, Experimental design and statistical models. *Archaeometry,* 41: 339–364.

Hasiotis, S. T., and Bown, T. M. 1992. Invertebrate trace fossils: The backbone of continental ichnology. In Maples, C.G., and West, R.R. (eds.), *Trace Fossils: Paleontological Society Short Courses*, No. 5, p. 64–104.

Helm, C. W. 2023. Pleistocene vertebrate trace fossils from the Cape south coast of South Africa: inferences and implications. Ph. D. thesis, Nelson Mandela University, 400 pp.

Helm, C. W., and Lockley, M. G. 2021. Pleistocene reptile swim traces confirmed from South Africa's Cape south coast. *South African Journal of Science,* 117(3/4): 8830. https://doi.org/10.17159/sajs.2021/8830

Final published version is available at
https://www.tandfonline.com/doi/full/10.1080/10420940.2023.2250062?src=recsys
Supplementary data is presented at the end of this document

Helm, C. W., McCrea, R. T., Cawthra, H. C., Thesen, G. H. H., and Mwankunda, J. M. 2018. Late Pleistocene trace fossils in the Goukamma Nature Reserve, Cape south coast, South Africa. *Palaeontologia Africana,* 52: 89–101.

Helm, C. W., Cawthra, H. C., Hattingh, R., Hattingh, S., McCrea, R. T., and Thesen, G. H. H. 2019. Pleistocene trace fossils of Robberg Nature Reserve. *Palaeontologia Africana,* 54: 36–47.

Helm, C. W., Cawthra, H. C., Combrink, X., Helm, C .J .Z., Rust, R., Steer, W., and Van den Heever, A. 2020. Pleistocene large reptile tracks and probable swim traces on South Africa's Cape south coast. *South African Journal of Science,* 116(3/4): 6542. https://doi.org/10.17159/sajs.2020/6542

Helm, C. W., Lockley, M. G., Moolman, L., Cawthra, H. C., De Vynck, J. C., Dixon, M. G., Stear, W., and Thesen, G.H.H. 2021. Morphology of Pleistocene elephant tracks on South Africa's Cape south coast, and probable elephant trunk drag impressions. *Quaternary Research,* 105: 100–114.

Helm, C. W., Carr, A. S., Cawthra, H. C., De Vynck, J. C., Dixon, M. G., Lockley, M. G., Stear, W., and Venter, J. A. 2023a. Large Pleistocene tortoise tracks on the Cape south coast of South Africa. *Quaternary Research,* 112: 93–110.

Helm, C. W., Carr, A. S., Cawthra, H. C., Vynck, J. C., Dixon, M. G., Gräbe, P-J., Thesen, G. H. H., and Venter, J. A. 2023b. Tracking the extinct giant Cape zebra (*Equus capensis*) on the Cape south coast of South Africa. *Quaternary Research,* published online. https://doi.org/10.1017/qua.2023.1

Helm, C. W., Carr, A. S., Lockley, M. G., Cawthra, H. C., De Vynck, J. C., Dixon, M. G., and Stear, W. Dating the Pleistocene hominin ichnosites on South Africa's Cape south coast. *Ichnos*, in press.

Hembree, D. I., and Hasiotis, S. T. 2007. Biogenic structures produced by sand-swimming snakes: a modern analog for interpreting continental ichnofossils. *Journal of Sedimentary Research,* 77: 389–397

Himes, J.G. 2000. Burrowing ecology of the rare and elusive Louisiana pine snake, *Pituophis ruthveni* (Serpentes: Colubridae). *Amphibia-Reptilia,* 22: 91–101.

Kim, J.Y., and Lockley M.G. 2013. Review of dinosaur tail traces. *Ichnos,* 20: 129–141.

Kinlaw, A. 1999. A review of burrowing by semi-fossorial vertebrates in arid environments. *Journal of Arid Environments,* 41: 127–145.

Klappa, C. F. 1980. Rhizoliths in terrestrial carbonates: classification, recognition, genesis and significance. *Sedimentology,* 27: 613–629.

Liebenberg, L. 2000. *A Photographic Guide to Tracks and Tracking in Southern Africa*. Cape Town, Struik Publishers, 144 pp.

Lockley, M. G., Cawthra, H. C., De Vynck, J. C., Helm, C. W., McCrea, R. T., and Nel, R. 2019. New fossil sea turtle trackway morphotypes from the Pleistocene of South Africa highlight role of ichnology in turtle palaeobiology. *Quaternary Research,* 92: 626–640.

Lockley, M. G., Helm, C. W., Cawthra, H. C., De Vynck, J. C., and Perrin, M.R. 2021. Pleistocene golden mole and 'sand-swimming' trace fossils from the Cape coast of South Africa. *Quaternary Research,* 101: 169–186.

Loope, D. B. 2005. Abundant trace fossils of sand-swimming reptiles preserved in cross strata deposited high on the flanks of giant Jurassic dunes. *Geological Society of America Abstracts with Programs*, 37(7), p. 339.

Loope, D. B. 2006. Burrows dug by large vertebrates into rain-moistened Middle Jurassic sand dunes. *Journal of Geology,* 114: 753–762.

Loope, D. B. 2008. Life beneath the surfaces of active Jurassic dunes: burrows from the Entrada Sandstone of south-central Utah. *Palaios,* 23: 411–419.

Malan, J. A. 1989. *Lithostratigraphy of the Waenhuiskrans Formation (Bredasdorp Group).* South African Committee for Stratigraphy (SACS), Lithostratigraphic Series 8. Department of Mineral and Energy Affairs, Geological Survey, Pretoria.

Malan, J. A. 1991. *Lithostratigraphy of the Klein Brak Formation (Bredasdorp Group)*. South African Committee for Stratigraphy (SACS), Lithostratigraphic Series 13. Department of Mineral and Energy Affairs, Geological Survey, Pretoria.

Marean, C. W., Cowling, R. C., and Franklin, J. 2020. The Palaeo-Agulhas Plain: temporal and spatial variation in an extraordinary extinct ecosystem of the Pleistocene of the Cape Floristic Region. In Cleghorn, N., Potts, A. J., Cawthra, H. C. (eds.), The Palaeo-Agulhas Plain: A Lost World and Extinct Ecosystem. *Quaternary Science Reviews,* 235: 106161. https://doi.org/10.1016/j.quascirev.2019.106161

Martin A. J. 2013. Life *Traces of the Georgia Coast*. Bloomington & Indianapolis, Indiana University Press, 670 pp.

Martin, L. D., and Bennett, D. K. 1977. The burrows of the Miocene beaver palaeocastor, Western Nebraska, U.S.A. *Palaeogeography, Palaeoclimatology, Palaeoecology,* 22(3): 173–193.

Matthews, N. A., Noble, T. A., and Breithaupt, B. H. 2016. Close-range photogrammetry for 3-D ichnology: the basics of photogrammetric ichnology. In Falkingham, P. L., Marty, D., Richter, A. (eds.), *Dinosaur Tracks: The Next Steps*. Bloomington, Indiana University Press, pp. 28–55.

Minter, N. J., and Braddy, S. J. 2006. The fish and amphibian swimming traces *Undichna* and *Lunichnium*, with examples from the Lower Permian of New Mexico, USA. *Palaeontology,* 49: 1123–1142.

Final published version is available at
https://www.tandfonline.com/doi/full/10.1080/10420940.2023.2250062?src=recsys
Supplementary data is presented at the end of this document

Minter, N.J ., and Braddy, S. J, 2009. Ichnology of an Early Permian intertidal flat: the Robledo Mountains Formation of southern New Mexico, USA. *Special Papers in Palaeontology* 82: 5–107. London, The Palaeontological Association. https://doi.org/10.1111/j.1475-4983.2009.00911.x

Minter, N. J., Lucas, S. G., Lerner, A. J., and Braddy, S. J. 2008. *Augerinoichnus helicoidalis*, a new helical trace fossil from the nonmarine Permian of New Mexico. *Journal of Paleontology,* 82(6): 1201–1206.

Roberts, D., and Cole, K. 2003. Vertebrate trackways in Late Cenozoic coastal eolianites, South Africa. Geological Society of America. Abstracts with Programs, XVI INQUA Congress, 70(3).

Roberts, D., Cawthra, H., and Musekiwa, C., 2013. Dynamics of late Cenozoic aeolian deposition along the South African coast: a record of evolving climate and ecosystems. Geological Society, London, Special Publications. https://doi.org/10.1144/SP388.11

Seilacher, A., 2008. Biomats, biofilms, and bioglue as preservational agents for arthropod trackways. *Paleogeography, Paleoclimatology, Palaeoecology*, 270(3–4): 252–257. https://doi.org/10.1016/j.palaeo.2008.07.011

Stuart, C., and Stuart, T. 2019. *A Field Guide to the Tracks and Signs of Southern and East African Wildlife*. Cape Town, Struik Nature, 488 pp.

Turek, V. 1989. Fish and amphibian trace fossils from Westphalian sediments of Bohemia. *Palaeontology,* 32: 623–643.

Uchman, A., Pika-Biolzi, M., and Hochuli, P. A. 2004. Oligocene trace fossils from temporary fluvial plain ponds: An example from the Freshwater Molasse of Switzerland. *Eclogae Geologicae Helvetiae,* 97: 133–148.

Final published version is available at
https://www.tandfonline.com/doi/full/10.1080/10420940.2023.2250062?src=recsys
Supplementary data is presented at the end of this document

Van den Heever, A., Mhlongo, R., and Benadie, K. 2017. *Tracker Manual – a Practical Guide to Animal Tracking in Southern Africa*. Cape Town, Struik Nature, 312 pp.

Waelbroeck, C., Labeyrie, L., Michel, E., Duplessy, J.C., Mcmanus, J.F., Lambeck, K., Balbon, E. and Labracherie, M., 2002. Sea-level and deep water temperature changes derived from benthic foraminifera isotopic records. Quaternary science reviews, 21(1-3), pp.295-305.

White, C. R. 2005. The allometry of burrow geometry. *Journal of Zoology,* 265: 395–403.

FIGURE CAPTIONS

FIG. 1. **A.** A puff adder employing rectilinear motion on a firm surface. **B.** A puff adder traceway on a Cape south coast modern dune surface - a combination of rectilinear and slight undulatory motion has been employed, and the central groove registered by the tail tip is evident in places; photo credit: Robin Catchpole. **C.** A central tai-tip drag impression is evident between raised curved features – a puff adder lunge was observed prior to the photograph being taken. **D.** Sidewinding traces of Péringuey's adder in the Namib Desert; direction of travel is from left to right (reproduced with permission from the Gobabeb Research & Training Centre). **E.** Péringuey's adder in the Namib Desert (reproduced with permission from the Gobabeb Research & Training Centre). **F.** An undulatory snake trace on a dirt road; scale bars = 10 cm.

FIG. 2. A puff adder registered these unusual traces in struggling to ascend and cross a rippled modern dune slope on the Cape south coast; impressions made by ventral scales are evident at lower left. Photo credit: Robin Catchpole.

FIG. 3. Sites mentioned in the text are shown, along with the extent of Cenozoic deposits and the extent of Namib dunes (De Cauwer 2007).

Final published version is available at
https://www.tandfonline.com/doi/full/10.1080/10420940.2023.2250062?src=recsys
Supplementary data is presented at the end of this document

FIG. 4. **A.** The loose track-bearing slab at Site 1 at the time of identification. **B.** Three weeks after initial identification, the slab was covered by a layer of algae, and sand and shell debris – scale bar = 10 cm. **C.** Long-horned buffalo (*Syncerus antiquus*) trackway at Site 1 – scale bar = 13 cm. **D.** 3D photogrammetry image of the trackway shown in (c) - horizontal and vertical scales are in metres. In **C** and **D** it is evident that the buffalo tracks are deeper than the snake traceway.

FIG. 5. **A.** Long, linear furrow at Site 1, crossed at an angle by the long-horned buffalo trackway; geological hammer for scale, length = 33 cm. **B.** One of the bovid tracks impinges on and slightly deforms the furrow; the narrow central groove can be seen in places within the furrow; scale bar = 13 cm. **C.** When the surface was covered in algae and sand, the narrow central groove was accentuated at the southern end of the slab; scale bars = 10 cm. **D.** 3D photogrammetry image of the snake traceway, showing slight sinuosity; horizontal and vertical scales are in metres.

FIG. 6. **A.** The curved groove feature at Site 2; rims are evident on both sides of the groove – scale bar = 10 cm. B**.** 3D photogrammetry image of the Site 2 feature; horizontal and vertical scales are in metres.

FIG. 7. **A.** The Site 3 surface and enigmatic ichnological features – scale bar = 10 cm. **B.** 3D photogrammetry image of the Site 3 surface; horizontal and vertical scales are in metres.

FIG. 8. **A** and **B**. *Augerinoichnus helicoidalis*, reproduced with permission from Minter et al. (2008); scales = 10 cm.

FIG. 9. *Serpentichnus robledoensis* trace from the Permian from New Mexico, attributed to a lysorophian amphibian; scale is in cm; reproduced with permission from Nic Minter.

FIG. 10. **A.** The coastal setting of Site 4 – the bottom arrow indicates the large composite elephant track, and the top arrow indicates the site of the undulatory trace. **B.** The undulatory trace at Site 4 – scale bars =10 cm.

Final published version is available at
https://www.tandfonline.com/doi/full/10.1080/10420940.2023.2250062?src=recsys
Supplementary data is presented at the end of this document

FIG. 11. Map of the area around Site 1 (Puff adder trace) and the relationship between the trace locale and the reported luminescence dating samples. The locations of Section A (Fig. S1) at De Kelders Cave and Section B in the embayment immediately east of De Kelders Cave (Fig. S1) are shown.

TABLES

Table 1: Details of the luminescence dating measurements with the dose rate obtained using standard methods. A burial mean water content of 3 ± 3 % was applied following Helm et al. (in press). The Central Age Model (CAM) weighted mean equivalent dose (Galbraith et al., 1999) was used to calculate sample ages. *outliers removed prior to averaging (see Fig. S3) # estimated typical depth during burial (see supplementary text and Table S1).

Final published version is available at
https://www.tandfonline.com/doi/full/10.1080/10420940.2023.2250062?src=recsys
Supplementary data is presented at the end of this document

Supplementary File

Sample preparation

Two field sampling campaigns were undertaken in the De Kelders Cave environs. The first was in 2005 (ASC and MDB) where sample Shfd05025 (DK2005) was obtained by hammering a steel tube into a cleaned sedimentary section within the Pleistocene aeolianite immediately overlying the De Kelders Cave rockshelter (**Figure S1**). This pilot sample was prepared and measured at the University of Sheffield luminescence laboratory. These results guided a second sampling campaign in 2013 carried out by the late Dr Dave Roberts, which yielded samples Leic13025 through Leic13028 (DK2A, DK2B, DK4 & DK5). These were obtained by cutting blocks of intact aeolianite from sites above and to the east of De Kelders Cave (**Figures S1 and S2**). These blocks were painted black and broken up under red light in the University of Leicester laboratory. In both cases, this involved the extraction of sand-sized quartz (150-250 µm; **Table S1**) following standard methods (Wintle, 1997). In brief, this comprised treatment in 10% HCl to remove carbonates, treatment in 30% H_2O_2 to remove organic matter, wet sieving, density separation at 2.70 g cm^{-3} to remove heavy minerals and a 45-minute treatment in concentrated HF to etch the outer layers of the quartz grains (removing the alpha dosed material and K-feldspar grains). The samples were treated in HCl for a further hour, rinsed, dried and re-sieved to the original size range.

Instrumentation and equivalent dose measurement

The pilot data for Shfd05025 were generated in 2005 using 9 mm diameter multi-grain aliquots of quartz in the University of Sheffield luminescence dating laboratory using a Risoe DA12 TL/OSL reader equipped with a 150 W halogen lamp (for 80 seconds at 125°C) stimulation source with detection via a Hoya U-340 filter. Equivalent doses (D_e) were determined using a Single Aliquot Regeneration (SAR) protocol (Murray and Wintle, 2000, 2003; Wintle and Murray, 2006) comprising a 5 regeneration point sequence. This included a repeat (recycling) regeneration dose point and a zero-dose point. Feldspar contamination was checked with an IR depletion ratio and preheat temperature optimised at 200°C for 10s based on a preheat test. A dose recovery test produced a given to measured D_e ratio of 0.96 ± 0.05. The Leicester measurements were undertaken in 2014 using a DA20 TL/OSL reader using 2 mm diameter multi-grain aliquots of quartz. Optical stimulation was provided by blue LEDS (wavelength 470 nm, 40 seconds at 125°C), with detection via a Hoya U-340 filter. Laboratory irradiations were delivered by a calibrated ^{90}Sr beta source. Based on the success of the pilot data, equivalent doses were also determined using a SAR protocol, but with a 6 or 7 regeneration point sequence which incorporated a repeat (recycling) regeneration dose point, an IR depletion ratio regeneration point (Duller, 2003) and a zero-dose point. Based on a suite of preheating dose recovery experiments, preheat combinations of 240/160°C (for L_x and T_x respectively) for Leic13025 and Leic13026, and 200/160°C for Leic13027 and Leic13028 were used (**Figure S3**).

For all data, aliquots were rejected from the analyses, prior to calculation of the sample equivalent dose if: 1) recycling ratios were outside of 10% of unity, 2) recuperation (zero dose) L_x/T_x values were greater than 5% of the natural sensitivity-corrected OSL signal, 3) there was a significant reduction in the sensitivity-corrected OSL signal after infra-red stimulation (Duller, 2003). All samples were analysed using the latest version (4.57) of the Risoe *Analyst* software (Duller, 2007). For the Leicester samples the OSL signal integration windows comprised the first 0.8 seconds of stimulation

with a background subtraction from the last 3.2 seconds of measurement. For Shfd05025 the first 0.96 seconds and last 3.2 seconds of the stimulation time were used. The dose-response curves were fitted with single saturating exponential fits with D_e uncertainties calculated using Monte Carlo methods (1000 iterations; Duller 2007).

Overall, the samples consistently indicated that they were well-suited to the SAR protocol. In all cases, dose recovery was within 10 % of unity (given measurement uncertainties) across a range of preheating temperatures (**Figure S3**), recycling ratios were consistently within 5% of unity and there was low signal recuperation (< 1 % of the natural OSL signal). There was no evidence of feldspar contamination. The D_e used for age calculation was determined using the Central Age Model (Galbraith et al., 1999). In some cases, outliers (identified using nMAD (Clarkson et al. 2017) were removed prior to averaging. These outliers and the distribution of all accepted aliquots are shown in **Figure S4**. The uncertainty in equivalent dose estimate incorporates beta source calibration (3%), curve fitting, counting statistics and a systematic instrumental uncertainty of 1.5%.

Dose rate determination

Dose rates were determined from elemental concentrations obtained via inductively coupled plasma mass spectrometry (ICP-MS) for U and Th at either SGS laboratories Canada (Shfd05025) or the University of Leicester (Leic13025 to Leic13028). The concentrations of K were very low in all cases (**Table S2**). For Leic13025-Leic13028, K was determined via XRF (PANalytical Axios Advanced XRF spectrometer with a lower K_2O detection limit of 0.001 %). For Shfd05025 ICP-OES was used. The elemental concentrations of were converted to annual dose rates following Guerin et al. (2011), with corrections for grain size (Mejdahl 1979), water content (Aitken, 1985) and HF etching (Bell 1979). Final age uncertainties incorporate 3% relative uncertainties for dose rate conversion factors. Further verification of the dose rates was provided using GM-beta counting, applied to a powdered and dried sub-sample of the block materials (Bøtter-Jensen and Mejdahl, 1988; Jacobs and Roberts, 2015; **Table S2**).

The measured water contents of the cemented blocks (<0.5% for Leic13025-Leic13028) and 1.4% for the tube (Shfd05025) were not considered representative of the burial period due to a combination of recent exposure in the sedimentary section and water losses during transport of the samples. Instead, water contents of 3 ± 3% were assumed, an estimate in line with other aeolianites on the Cape south coast (for details see Helm et al. 2023). This uncertainty encompasses a range of water contents, allowing for fluctuations around the long-term burial water content. We also evaluated the impact of progressive carbonate cementation (and concomitant loss of pore water) on the evolution of the sample dose rates (following Mauz and Hoffmann, 2014). In this instance heavily cemented sample Leic13027 indicates the potential rapidity of cementation in this context (age 6.1 ± 0.4 ka). This rapid cementation is consistent with the arguments set out in Helm et al (2023) for the Cape south coast aeolianites more broadly. However, at De Kelders it was found that modelled ages assuming progressive cementation (formation of 25 ± 5 % by volume cement) and a reduction in water content from 4 ± 1 % to 2 ± 1 % over ~6 ka altered the ages very little. For example, the modelled age

for Leic13025 was 93 ± 7 ka compared to the unmodelled age of 93 ± 6 ka. For this reason, we report the conventionally derived OSL ages in the main text.

Cosmic dose rates were calculated using the *Luminescence* R package (Kreutzer et al., 2012, 2022) following the work of Prescott and Hutton (1994). Due to the low sedimentary dose rates in these samples the cosmic dose contribution is quite significant (32-50 % of the total dose rate; **Table S2**). To quantify this as best as possible, the reported values here are time-weighted means obtained using the sample depths relative to palaeosol 1 (which caps the Pleistocene aeolianite succession; **Figure S2**) and an estimate of the depth of the subsequent Holocene dune sand cover for the final ~6 ka of burial. A conservative 10% relative uncertainty was included with the cosmic dose rate to account for uncertainties in the thickness and duration (variability therein) of Holocene dune cover. The final ages are internally consistent (in stratigraphic order) and broadly consistent with the age of shore-proximal aeolianites elsewhere in this sector of the coastline (e.g. Carr et al., 2010; Bateman et al 2011).

REFERENCES

Aitken, M.J., 1985. *Thermoluminescence Dating*. Academic Press, London, 370 pp.

Bateman, M.D., Carr. A.S., Holmes, P.J., Dunajko, A., McLaren, S.J., Marker, M.E., Roberts, D.L, Murray-Wallace, C.V., Bryant, R.G. (2011) The evolution of barrier dune systems: A case study of the Middle-Late Pleistocene Wilderness barrier dunes, South Africa. *Quaternary Science Reviews* 30, 63-81.

Bell, W.T., 1979. Thermoluminescence dating: radiation dose rate data. *Archaeometry* 21,243–246.

Bøtter-Jensen, L., Mejdahl, V., 1988. Assessment of beta dose-rate using a GM multicounter system. *Nuclear Tracks and Radiation Measurements* 14, 187–191.

Carr, A.S., Bateman, M.D., Roberts, D.L., Murray-Wallace, C.V., Jacobs, Z., Holmes, P.J., 2010. The last interglacial sea-level high stand on the southern Cape coastline of South Africa. *Quaternary Research* 73, 351-362

Clarkson, C., Jacobs, Z., Marwick, B., Fullagar, R., Wallis, L., Smith, M., Roberts, R. G., Hayes, E., Lowe, K., Carah, X., Florin, S.A. 2017. Human occupation of northern Australia by 65,000 years ago. *Nature* 547, 306–310.

Duller, G.A.T., 2003. Distinguishing quartz and feldspar in single grain luminescence measurements. *Radiation Measurements* 37, 161–165.

Duller, G.A.T., 2007. Assessing the error on equivalent dose estimates derived from single aliquot regenerative dose measurements. *Ancient TL* 25, 15–24.

Galbraith, R.F., Roberts, R.G., Laslett, G.M., Yoshida H., Olley, J.M., 1999. Optical dating of single and multiple grains of quartz from Jinmium rock shelter, northern Australia, part 1, Experimental design and statistical models. *Archaeometry* 41, 339–364.

Final published version is available at
https://www.tandfonline.com/doi/full/10.1080/10420940.2023.2250062?src=recsys
Supplementary data is presented at the end of this document

Guérin, G., Mercier, N., Adamiec, G., 2011. Dose-rate conversion factors: update. *Ancient TL* 29, 5–8.

Helm, C.W., Carr, A.S., Lockley, M.G., Cawthra, H.C., De Vynck, J.C., Dixon, M.G., Stear, W. 2023 Dating the Pleistocene hominin ichnosites on South Africa's Cape south coast. *Ichnos.* 30, 49-68

Jacobs, Z. Wintle, A.G., Duller, G.A.T., 2003. Optical dating of dune sand from Blombos Cave, South Africa: I—multiple grain data. *Journal of Human Evolution* 44, 599–612.

Kreutzer, S., Burow, C., Dietze, M., Fuchs, M., Schmidt, C., Fischer, M., Friedrich, J., Mercier, N., Philippe, A., Riedesel, S., Autzen, M., Mittelstrass, D., Gray, H., Galharret, J., 2022. Luminescence: Comprehensive Luminescence Dating Data Analysis. R package version 0.9.19, https://CRAN.R-project.org/package=Luminescence

Kreutzer, S., Schmidt, C., Fuchs, M.C., Dietze, M., Fischer, M., Fuchs, M., 2012. Introducing an R package for luminescence dating analysis. *Ancient TL* 30, 1-8.

Mejdahl, V., 1979. Thermoluminescence dating - Beta-dose attenuation in quartz grains. *Archaeometry* 21, 61–72.

Mauz, B., Hoffmann, D., 2014. What to do when carbonate replaced water: RCarb, the model for estimating the dose rate of carbonate-rich samples. *Ancient TL* 32, 24–32.

Murray, A.S., Wintle, A.G., 2000. Luminescence dating of quartz using an improved single-aliquot regenerative-dose protocol. *Radiation Measurements* 32, 57–73.

Murray, A.S., Wintle, A.G., 2003. The single-aliquot regenerative-dose protocol: potential for improvements in reliability. Radiation Measurements 37, 377–381.

Prescott, J.R., Hutton, J.T., 1994. Cosmic ray contributions to dose rates for luminescence and ESR dating: large depths and long-term variations. *Radiation Measurements* 23, 497–500.

Vermeesch, P., 2009. RadialPlotter: a Java application for fission track, luminescence and other radial plots. *Radiation Measurements* 44, 409–41.

Wintle, A.G. 1997. Luminescence dating: laboratory procedures and protocols. *Radiation Measurements* 27, 769–817.

Wintle, A.G., Murray, A.S., 2006. A review of quartz optically stimulated luminescence characteristics and their relevance in single-aliquot regeneration dating protocols. *Radiation Measurements* 41, 369–391.

Final published version is available at
https://www.tandfonline.com/doi/full/10.1080/10420940.2023.2250062?src=recsys
Supplementary data is presented at the end of this document

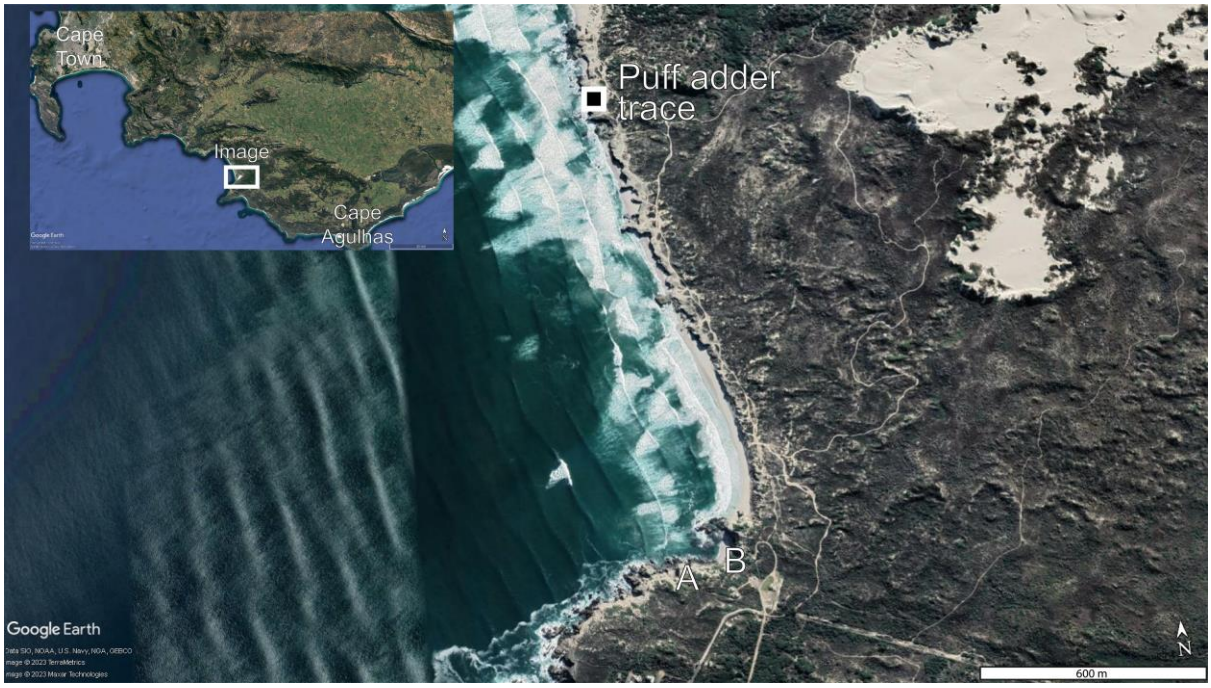

Figure S1: Map of the area around Site 1 (Puff adder trace) and the relationship between the trace locale and the reported luminescence dating samples. The locations of section **A** (**Figure S2**) at De Kelders Cave and Section **B** in the embayment immediately east of De Kelders Cave (**Figure S2**) are shown.

Final published version is available at
https://www.tandfonline.com/doi/full/10.1080/10420940.2023.2250062?src=recsys
Supplementary data is presented at the end of this document

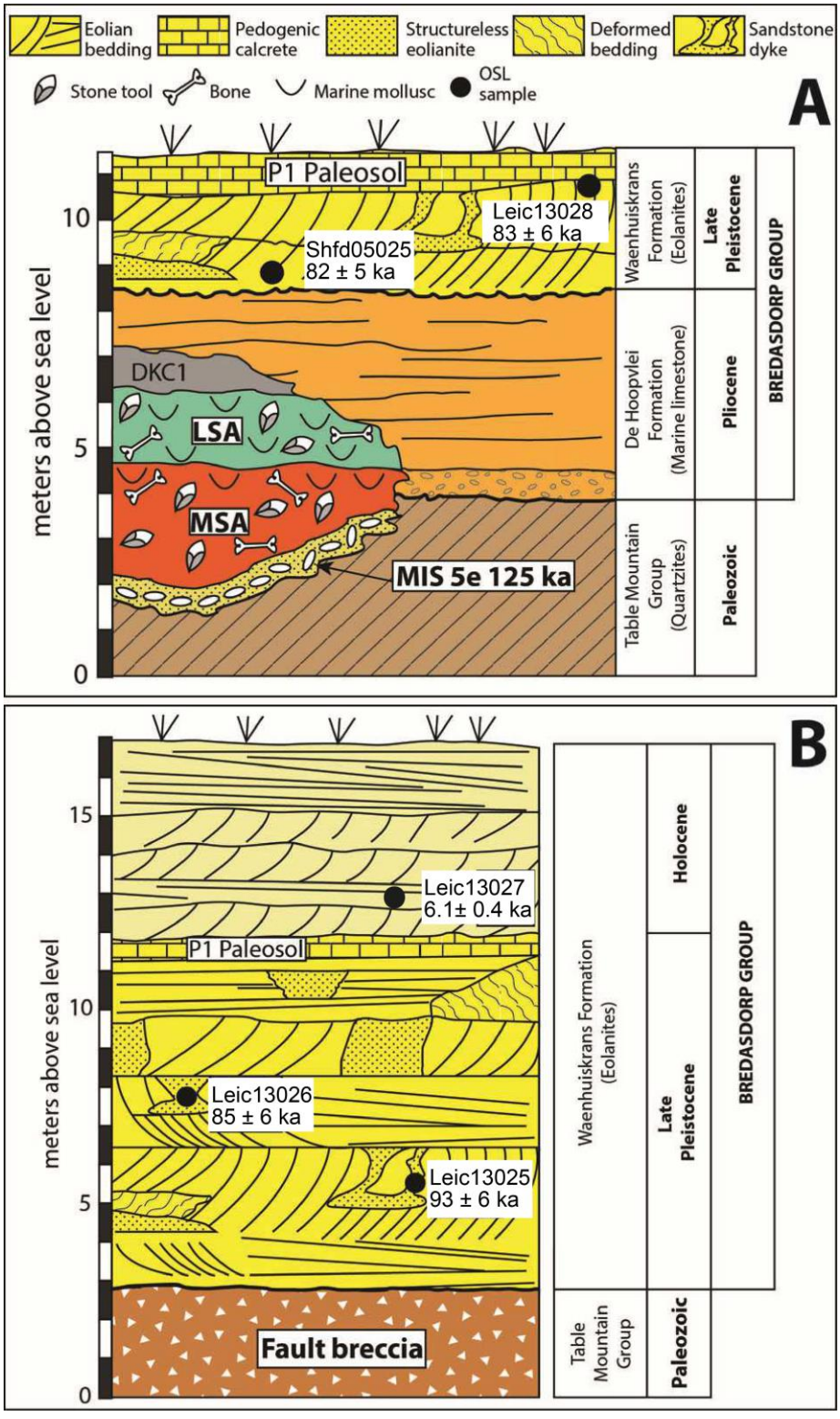

Figure S2: Stratigraphic sections for the two sample locales. The depths and ages for the five OSL samples are indicated.

Final published version is available at
https://www.tandfonline.com/doi/full/10.1080/10420940.2023.2250062?src=recsys
Supplementary data is presented at the end of this document

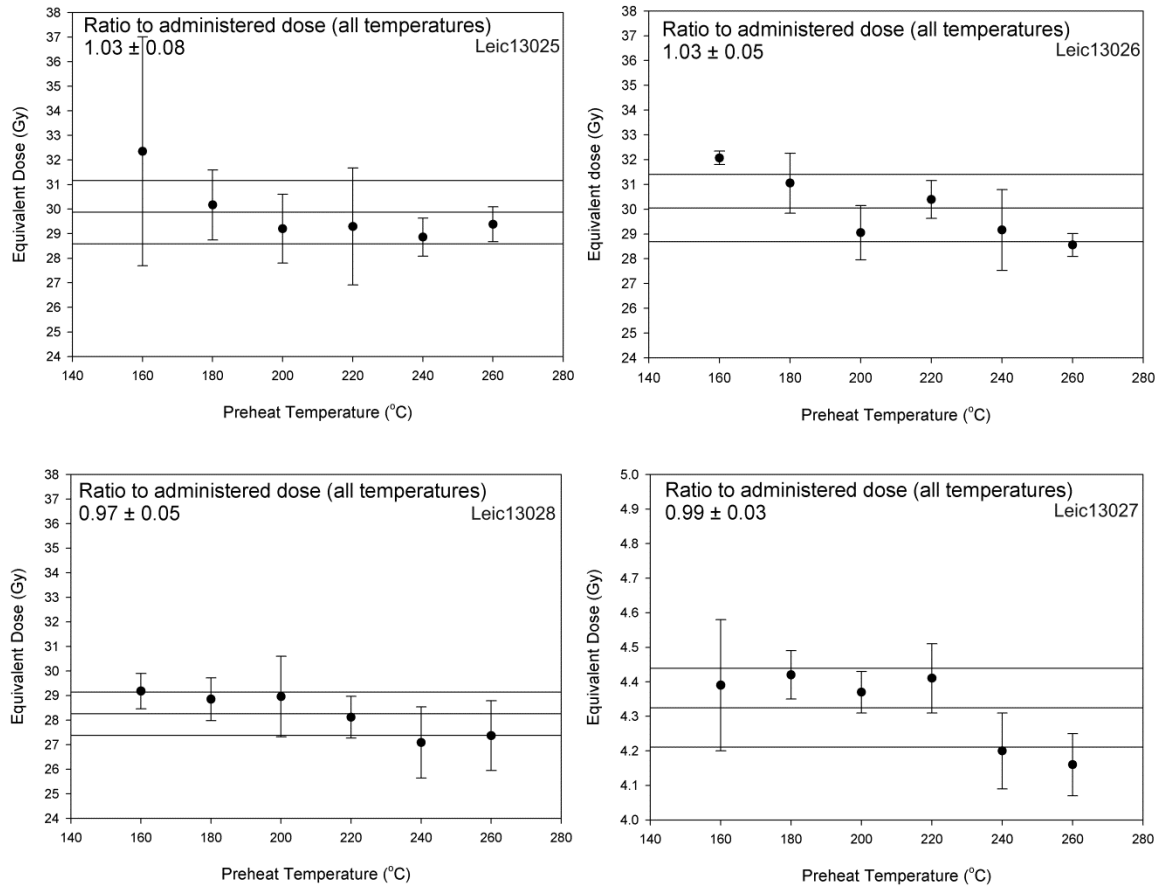

Figure S3: The results of dose recovery experiments for Leic13025, Leic13026, Leic13027 and Leic13028. The horizontal lines show the mean equivalent dose (and one standard deviation) for the full data set, while each data point is the average and standard deviation of three measured aliquots. The administered laboratory beta doses were 29 Gy for all samples, except Leic13027, which was 4.4 Gy.

Final published version is available at
https://www.tandfonline.com/doi/full/10.1080/10420940.2023.2250062?src=recsys
Supplementary data is presented at the end of this document

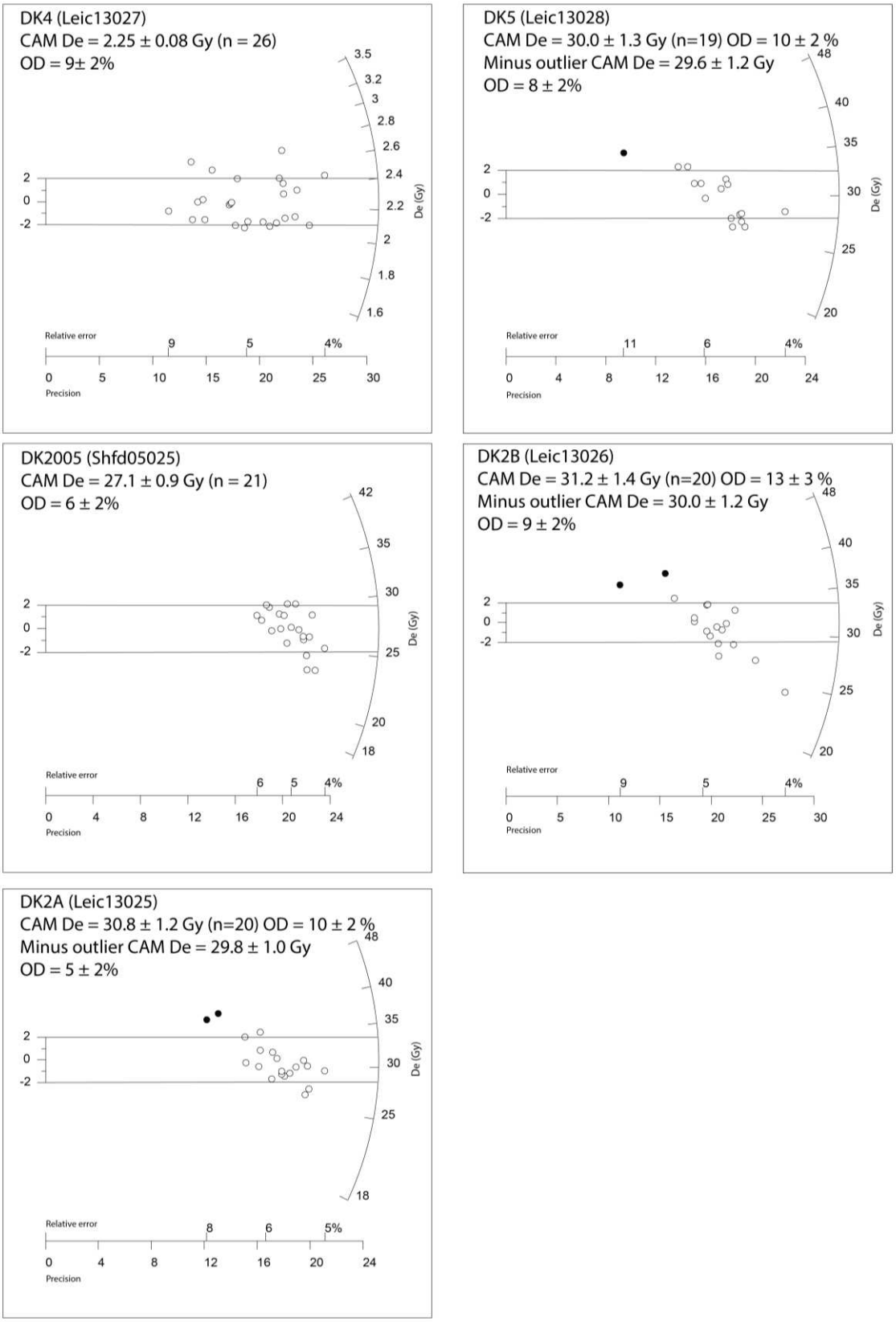

Figure S4: Radial plots for the five reported samples (created using the Radial Plotter software; Vermeesch (2009)) with determined outliers shown in black.

Final published version is available at https://www.tandfonline.com/doi/full/10.1080/10420940.2023.2250062?src=recsys
Supplementary data is presented at the end of this document

Table S1: Details of the luminescence dating measurements with the dose rate obtained using standard methods. A burial mean water content of 3 ± 3 % was applied following Helm et al. (2023). The Central Age Model (CAM) weighted mean equivalent dose (Galbraith et al., 1999) was used to calculate sample ages. *outliers removed prior to averaging (see **Figure S2**) # estimated typical depth during burial (see text and **Table S2**).

Lab code	Field code	Burial depth (m)#	Measured water content (%)	Applied water content (%)	Grain size (µm)	Aliquots accepted / measured	CAM D_e (Gy)	OD (%)	Total dose rate (Gy ka^{-1})	Age (ka)
Leic13027	DK4	3.5	0.2	3 ± 3	212-250	26/26	2.25 ± 0.08	9 ± 2	0.37 ± 0.02	**6.1 ± 0.4**
Leic13028	DK5	2	0.5	5 ± 3	180-250	16/19	29.6 ± 1.2	8 ± 2	0.35 ± 0.03	**83 ± 6**
Shfd05025	DK2005	4.5	1.4	3 ± 3	180-250	21/22	27.1 ± 0.9	6 ± 2	0.33 ± 0.09	**82 ± 5**
Leic13026	DK2B	8	0.2	3 ± 3	180-212	20/20	30.0 ± 1.2*	9 ± 2	0.37 ± 0.02	**85 ± 6**
Leic13025	DK2A	10	0.3	3 ± 3	150-250	20/20	29.8 ± 1.0*	5 ± 2	0.32 ± 0.02	**93 ± 6**

Final published version is available at https://www.tandfonline.com/doi/full/10.1080/10420940.2023.2250062?src=recsys
Supplementary data is presented at the end of this document

Table S2: Details of the measured elemental concentrations and dose rate calculations. [a]an internal alpha dose rate was included following Jacobs et al. (2003). Relative uncertainties of 10% (U and Th) and 5% (K) were applied to the elemental concentrations and were propagated to the final dose rate uncertainties. External gamma and beta doses were corrected for water content (Aitken, 1985), external beta doses were also corrected for grain size (Mejdahl, 1979) and HF etching (Bell, 1979). The external beta dose rates were verified using GM beta counting on a dried and powdered sub-sample (Bøtter-Jensen and Mejdahl, 1988; Jacobs and Roberts, 2015). Cosmic dose rates were calculated using the *Luminescence* R package (Kreutzer et al., 2012, 2022) following Prescott and Hutton (1994). The reported values are weighted means based on the cosmic dose to the sample depth within Pleistocene aeolianite relative to the overlying palaeosol, and then an additional cover of Holocene dune sand for the last 6 ka. A conservative 10% relative uncertainty has then been applied.

Lab code		**U (ppm)**	**Th (ppm)**	**K (%)**	**Internal alpha dose rate (Gy ka^{-1})[a]**	**External beta dose rate (ICP-MS) (Gy ka^{-1})**	**External gamma dose rate (Gy ka^{-1})**	**Cosmic dose rate (Gy ka^{-1})**	**Total Dose rate (Gy ka^{-1})**
Leic13027	DK4	0.61	0.60	0.03	0.036 ± 0.01	0.096 ± 0.007	0.100 ± 0.006	0.139 ± 0.014	0.37 ± 0.02
Leic13028	DK5	0.30	0.50	0.04	0.036 ± 0.01	0.069 ± 0.005	0.066 ± 0.004	0.183 ± 0.018	0.35 ± 0.02
Shfd05025	DK2005	0.36	0.40	0.06	0.036 ± 0.01	0.085 ± 0.006	0.072 ± 0.005	0.138 ± 0.014	0.33 ± 0.02
Leic13026	DK2B	0.61	0.3	0.06	0.036 ± 0.01	0.111 ± 0.007	0.094 ± 0.006	0.128 ± 0.013	0.37 ± 0.02
Leic13025	DK2A	0.54	0.6	0.03	0.036 ± 0.01	0.090 ± 0.006	0.093 ± 0.091	0.104 ± 0.010	0.32 ± 0.02
						External beta dose rate: GM beta counting (Gy ka^{-1})			
Leic13027	DK4					0.09 ± 0.01			
Leic13028	DK5					0.05 ± 0.01			
Shfd05025	DK2005					Nd.			
Leic13026	DK2B					0.09 ± 0.02			
Leic13025	DK2A					0.08 ± 0.01			